Analysis of Time of Arrival Estimation Using Wideband Measurements of Indoor Radio Propagations

Nayef Alsindi, *Student Member, IEEE*, Xinrong Li, *Member, IEEE*, and Kaveh Pahlavan, *Fellow, IEEE*

***Abstract*—Using time of arrival (TOA) to determine the distance between the transmitter and the receiver is the most popular technique for accurate indoor positioning. The accuracy of measuring the distance using this method is sensitive to the bandwidth of the system and the multipath condition between the wireless terminal and the access point. In general, as the bandwidth increases beyond a certain value, it is expected that the measured TOA error approaches zero. However, for the so-called undetected direct path (UDP) conditions, the system exhibits substantially high distance measurement errors that cannot be eliminated with the increase in the bandwidth of the system. In this paper, we provide an analysis of the behavior of superresolution and traditional TOA estimation algorithms in line-of-sight (LOS), non-LOS, and UDP conditions in indoor areas. The analysis is based on wideband frequency-domain measurements of the indoor radio channel propagations in several indoor areas, with special attention to the UDP conditions.**

***Index Terms*—Direct path blockage, indoor geolocation, non-line-of-sight (NLOS) geolocation, superresolution algorithms, time-of-arrival (TOA) estimation, undetected direct path (UDP), wideband channel measurement.**

I. Introduction

In RECENT years, a growing interest in location-finding systems has emerged for various geolocation applications. Two existing location-finding systems, namely, the Global Positioning System (GPS) and wireless enhanced 911 (E-911), have been used to provide relatively accurate positioning for the outdoor environment [1]. These technologies, although accurate, could not provide the same accuracy when applied to indoor positioning. The different physical requirements of the indoor environment necessitate alternative systems to provide accurate positioning. Therefore, the design and development of indoor positioning systems require in-depth modeling of the indoor wireless channel.

Manuscript received October 21, 2004; revised April 18, 2007. This paper was presented in part at the Wireless Communications and Networking Conference, Atlanta, GA, March 2004.

N. Alsindi and K. Pahlavan are with the Center for Wireless Information Network Studies, Department of Electrical and Computer Engineering, Worcester Polytechnic Institute, Worcester, MA 01609 USA (e-mail: nalsindi@wpi.edu; kaveh@wpi.edu).

X. Li was with the Center for Wireless Information Network Studies, Department of Electrical and Computer Engineering, Worcester Polytechnic Institute, Worcester, MA 01609 USA. He is now with the Department of Electrical Engineering, University of North Texas, Denton, TX 76203 USA (e-mail: xinrong@unt.edu).

Color versions of one or more of the figures in this paper are available online at http://ieeexplore.ieee.org.

Digital Object Identifier 10.1109/TIM.2007.904481

Although many wideband radio propagation models for telecommunication application exist in the literature, their relevance to geolocation systems is distant [2]. In telecommunication applications, the critical parameters are the distance-power gradient and the multipath delay spread of the channel [3]. However, in geolocation applications, the parameters of interest are the relative power and the estimated time of arrival (TOA) of the direct line-of-sight (DLOS) path. Therefore, the accuracy of the measurement and modeling of these parameters limits the achievable performance of indoor geolocation systems. However, due to severe multipath conditions and the complexity of radio propagation, the DLOS path cannot always be accurately detected [2], [4]. Improving its detection and TOA estimation requires improving the time-domain resolution of the channel response to resolve the multipath and enhance the accuracy of estimation.

Spectral estimation methods, namely, superresolution algorithms, have been recently used by a number of researchers for time-domain analysis of different applications [5], [6]. Specifically, they have been employed in the frequency domain to estimate multipath time-dispersion parameters, such as mean excess delay and root mean square (RMS) delay spread [7]. In addition, [8] used superresolution algorithms to model indoor radio propagation channels with parametric harmonic signal models. Recently, however, superresolution algorithms have been applied to accurate TOA estimation for indoor geolocation with diversity combining schemes [9]. The MUltiple SIgnal Classification (MUSIC) algorithm was used as a superresolution technique, and it was shown to improve TOA estimation.

In indoor positioning, the behavior of TOA estimation in different environments is another important factor in determining the performance of geolocation systems. Besides physical classification of line-of-sight (LOS) versus non-LOS (NLOS), [2] has shown that there exists further classification that depends on the channel profile and the characteristics of the DLOS path. The first category of this classification is the dominant direct path (DDP), where the DLOS path is detected and it is the strongest. The second category is the non-DDP (NDDP), where the DLOS path is detected but it is not the strongest. The last category is the undetected direct path (UDP), where the DLOS path is undetected.

This paper presents the results of a measurement campaign that was created for the classification of channel profiles, with emphasis on finding more UDP cases. The performance and behavior of the distance error, which is directly related to

0018-9456/$25.00 © 2007 IEEE

the TOA estimation error, is analyzed in all of these different scenarios. In addition, the performance of different TOA estimation algorithms, namely, the inverse Fourier transform (IFT), direct-sequence spread spectrum (DSSS), and superresolution eigenvector (EV) algorithms, is compared for different environments and bandwidths. The classification of channel profiles and the performance analysis that are presented in this paper provide a deeper insight into wireless channel modeling for indoor geolocation.

This paper is organized as follows: Section II describes the indoor channel characteristics. Section III describes the procedure and instrumentation that was used to measure the different indoor channel profiles. Section IV introduces the TOA estimation algorithms that we studied. Section V provides performance evaluation of the different algorithms in different environments and bandwidths. The conclusion is provided in Section VI.

II. Indoor Channel Characterization for TOA Estimation

Wideband radio propagation channel modeling for indoor geolocation application requires examining the channel profiles in different environments. The behavior of the channel profile or, specifically, the TOA of the DLOS path depends on the physical location of the receiver with respect to the transmitter. In this section, two classification schemes that are based on the channel profile of the measurement data are discussed. Then, the UDP phenomenon will be examined in more detail.

A. Classification Based on Physical Characteristics

One of the major classifications in the study of channel modeling is based on the physical properties of the indoor environment. LOS and NLOS are easily distinguishable from the measurement scenario. In the former, both the transmitter and the receiver have no physical obstructions between them, enabling accurate TOA estimation of the DLOS path. In the latter, however, the obstruction, which is usually one to several walls or other objects such as cabinets or elevators, further degrades the accuracy of the estimation. In fact, for some cases, the DLOS path is undetectable, causing a major ranging error.

B. Classification Based on Measurement Characteristics

The second classification is based on the measured channel characteristics that are apparent in the time-domain profile. Regardless of physical obstructions, the measurement is classified according to the availability and the power of the TOA of the DLOS path. For this classification, a threshold was used to identify if the DLOS path is detected or not. The method in computing and implementing this threshold is discussed in more detail in the measurement section. DDP is the easiest to detect from the profile, as shown in Fig. 1(a), because it has a distinct strong DLOS path, which enables receivers to lock onto it and estimate the TOA accurately. When the power of the DLOS path gets weaker and is no longer the strongest, then the channel characteristics fits in the NDDP category, which is shown in Fig. 1(b). For this case, the significant loss of accuracy in TOA estimation can be reduced when a more complex RAKE receiver is used to resolve the multipath. In Fig. 1(c), when the DLOS path power falls below the threshold and is therefore undetected, the channel condition is classified as UDP. In this unfavorable situation, neither the GPS nor the RAKE receiver can accurately detect the TOA, and this, specifically, causes the most significant error in indoor positioning applications. As a result, it is important to understand how and why UDP situations arise in indoor environments. The succeeding sections attempt to shed some light on this rather important case, where a measurement campaign was set up to better analyze and understand this situation.

C. UDP Challenge

With these different channel characteristics described, UDP poses the most significant challenge to limiting the accuracy of indoor geolocation systems. For reliable geolocation in indoor environments, it is necessary to identify and mitigate (if possible) range estimates that are corrupted by UDP error. Localization algorithms that operate without knowledge of the channel condition will face substantial performance degradation.

A measured channel profile that describes the characteristics of the UDP case is shown in Fig. 1(c). It is clear that the other paths have significant power when compared with the DLOS path. This relative power drop is beyond the dynamic range of the measurement system. In most cases, this is caused by the existence of a metallic obstruction in the direct path. In other instances, there might be a number of walls that attenuate the DLOS path considerably, relative to the other paths. In both cases, the paths arriving from other directions are much stronger.

In situations where UDP is unavoidable, the next step is to find ways to resolve it or reduce its effect on TOA estimation. One way is to apply estimation algorithms to try to resolve the multipath and perhaps reduce the error in UDP conditions. A second approach might consider the bandwidth of the system. In many cases, when the bandwidth of the system increases, the time-domain resolution and, thus, the accuracy of TOA estimation increase. Both the use of estimation algorithms and the system bandwidth will be discussed later, and its effect on the TOA estimation error will be analyzed.

The special case of UDP did not receive significant attention in the past, and the previous measurements were classified according to LOS and NLOS. As a result, a measurement campaign was created to collect more UDP measurements for statistical analysis. Before that, a description of the measurement system and the measurement database that was used in the analysis will provide both clarification and justification for the measurement approach that we employed.

III. Measurement of Different Channel Profile Classes

A. Measurement System

One of the most popular techniques for experimentally calculating the TOA is through the use of the frequency-domain

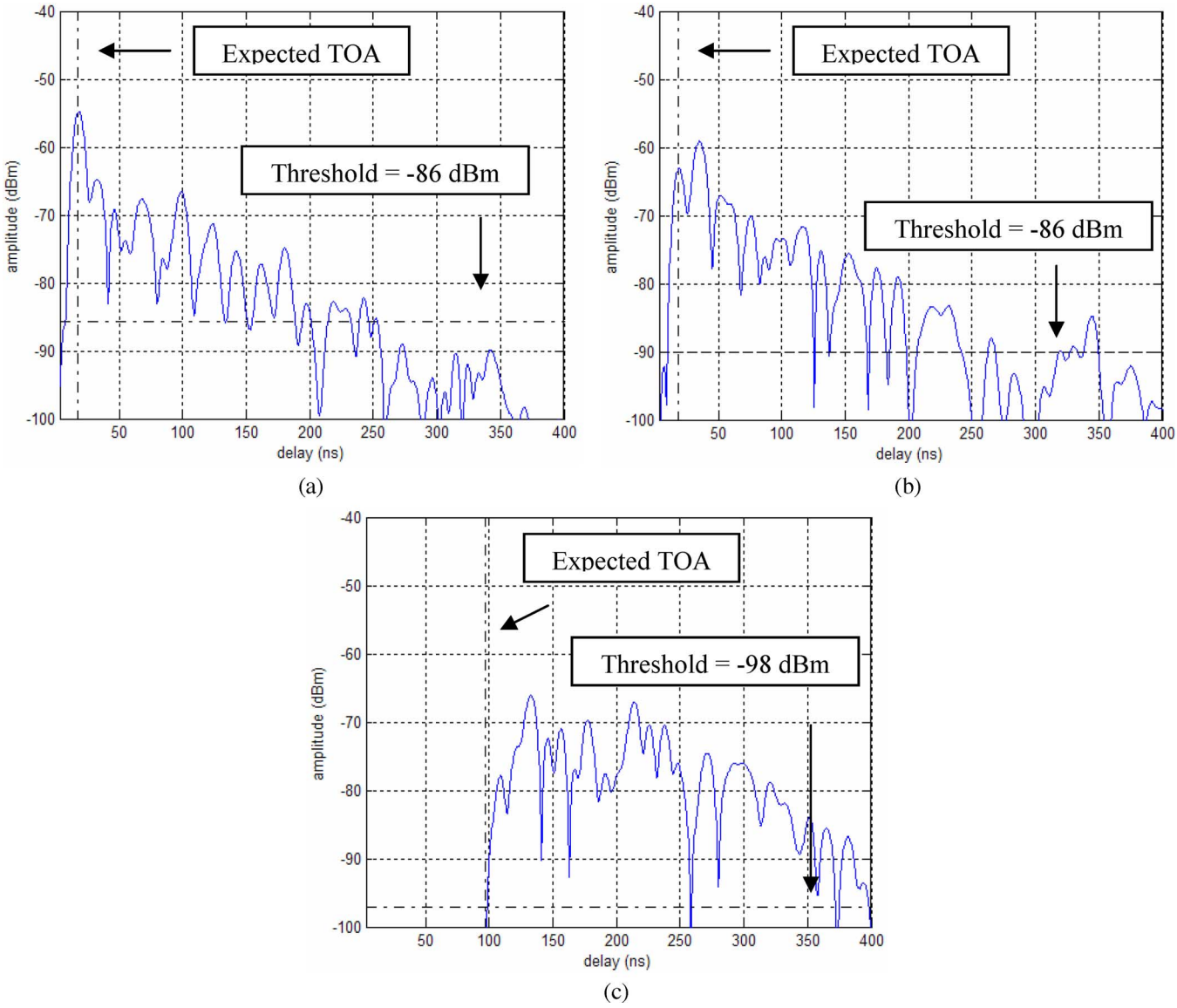

Fig. 1. Sample of measured indoor channel profiles. (a) DPP. (b) NDDP. (c) UDP.

measurement system that was described in [10]. The main component of this system is a network analyzer that sweeps the channel from 900 to 1100 MHz. After passing through a 30-dB amplifier, the output is connected to the transmitter antenna by a cable. The receiver is connected to an attenuator and then to the receiver port of the network analyzer. Both antennas are 1-GHz monopole quarter-wave adjusted on square plates. The analyzer has a sensitivity of -100 dBm. The measurements are further calibrated to remove the effects of the lossy cables, power amplifiers, and other system imperfections. The frequency-domain measurements were conducted by fixing the transmit antenna and moving the receiver around the desired locations. After data collection, the measured frequency-domain data are passed through a Hanning window to further suppress the unwanted sidelobes. Then, the IFT is applied to estimate the time-domain channel profile. As mentioned earlier, a threshold is used to characterize the channel profile according to the power of the DLOS path. Estimating the time-domain power delay profile requires estimating the relative amplitudes and delays of the arriving multipath components. Distinguishing between actual paths and measurement system noise required the implementation of a noise threshold. Since the noise floor of the measurement system is -100 dBm and the Hanning window has sidelobes of -31 dB below the peak of the profile, a threshold is selected according to the larger value of the two. Then, the first path that has power greater than the noise threshold is the first detected path.

B. Measurement Database

A measurement database was created by combining previous measurements that were produced by the Center for Wireless Information Network Studies (CWINS) and recent measurements that were conducted on the third floor of the Atwater Kent (AK) Laboratories, Department of Electrical Engineering, Worcester Polytechnic Institute (WPI). The previous measurements include LOS measurements that were taken on the second and third floor of AK reported in [11] and, mainly, NLOS

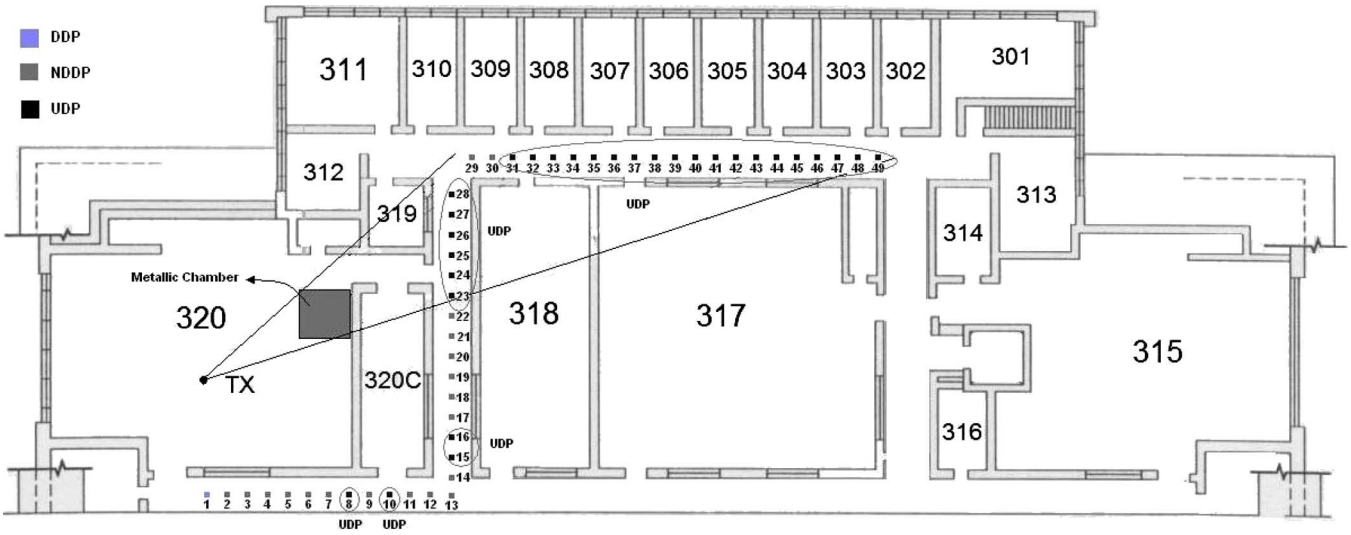

Fig. 2. Setup 1 measurement campaign on the third floor of AK.

measurements reported in [12]. After analyzing and classifying these measurements, it was apparent that they lacked sufficient UDP cases for statistical analysis, where they contained only 16 measurements. Therefore, the recent measurement campaign was also conducted on the third floor of AK, with special attention to the generation of more UDP cases. To analyze the behavior of the DLOS path in such unfavorable conditions, it was necessary to create a database that is tailored to this kind of classification.

The search for UDP required thorough analysis of transmitter–receiver locations within the building to vary the attenuation effect on the DLOS path and examine its effect on the channel profile. The recent campaign produced 105 measurement points. Fifty-two of those measurement locations are UDP, another 52 are NDDP, and only one measurement point is DDP. The measurement database is used in analyzing the performance of different estimation algorithms under those different multipath conditions. Including the earlier reported CWINS measurements, a total of 256 measurements were collected, of which 71 are LOS and 185 are NLOS. Overall, the database contains a total of 68 UDP measurement points, along with 100 NDDP and 88 DDP points that were used for statistical analysis.

C. Measurement of UDP Condition

The measurements were conducted on the third floor of the AK building at WPI. The AK building was built in 1906 and had two major remodeling and additions in 1934 and 1981. Therefore, in some areas within the building, there is more than one exterior-type wall. The exterior walls of this building are made of heavy brick, the interior walls are made of aluminum studs and sheet rock, the floors are made of metallic beams, the doors and windows are metallic, and many other metallic objects are spread over different laboratory areas. The excessive number of metallic objects and internal walls makes this building a very harsh environment for radio propagation.

The measurement campaign is based on two measurement setups that approach the possibility of UDP occurrence differently. In setup 1, a deterministic approach is followed, where the selected receiver measurement points were expected to exhibit UDP characteristics because of the physical geometry and the actual obstruction in the DLOS path. In setup 2, a more random approach was followed, as several measurement points were taken, but their nature was not expected in advance. The actual distance between the transmitter and receiver is physically measured and later compared with the estimated distance.

Setup 1 took advantage of a metallic chamber, which is better known as the Faraday Chamber, residing in the CWINS Laboratory (AK320). The transmitter was placed inside the laboratory, and the receiver was moved around it through the corridors. Fig. 2 shows the third floor plan of AK building, along with the location of the transmitter and receiver points for setup 1. Notice the metallic chamber that is designated by gray shading in the figure. The receiver points that are shown in the figure were taken 1 m apart. This helped to provide closely spaced snapshots of the channel profile as the receiver moves from one point to the next.

Prior to conducting the measurements, it was desired to see what happens to the DLOS path as the receiver moves in a straight line from one point to another. Specifically, the pattern in which the channel might switch between the three different classifications would provide further insight into the nature of the problem. The expectations for this part of the measurement campaign were as follows: The occurrence of UDP would be localized to the region that is shadowed by the metallic chamber, as shown in Fig. 2. In addition, it was expected that the other measurement points that were not covered by the UDP region would most likely exhibit NDDP characteristics.

After conducting the measurements and analyzing their channel characteristics, the outcome is interesting. In Fig. 2, the light dots represent NDDP measurement points, while the dark ones represent UDP. As expected, the region that was shadowed by the chamber exhibited UDP characteristics. There are two points, however, in this region that appeared as NDDP. A possible explanation for this could be that, since these two points are located exactly around the corner of the corridor,

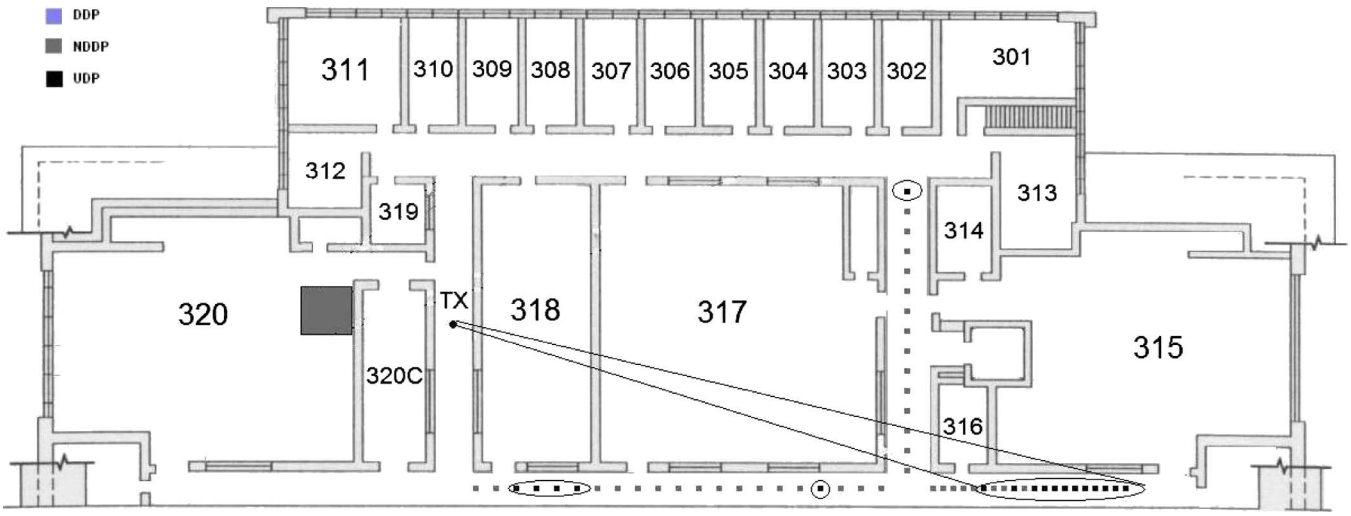

Fig. 3. Setup 2 measurement campaign on the third floor of AK.

the diffracted path is very close to the direct path, and this might have appeared to be a stronger DLOS path than expected. Another interesting observation is that, in addition to the region that was affected by the chamber, there are four UDP points that occurred in the corridor around the CWINS laboratory. This is an indication that this unfavorable condition occurs in different locations because of metallic objects or other obstructions that are not accounted for. All in all, from this particular measurement setup, 60% of the points are UDP, and the majority of these were the outcome of the metallic chamber.

Fig. 3 shows the location of the transmitter and receiver points for setup 2. The transmitter was fixed in the corridor to the right of AK320, and the receiver was moved to different points around the adjacent corridors. Contrary to the earlier setup, the outcome of this approach was not known in advance, and in addition, fewer UDP points were expected. However, after analysis, a substantial number of UDP points, i.e., about 32% of the measurements, were measured at different locations. In some cases, UDP occurs between NDDP points; in other cases, it occurs one after the other. For the former case, this is mainly because of shadow fading that is caused by obstacles, in addition to walls, that suddenly attenuate the DLOS path power significantly. However, for the latter case, the walls are the main contributors to the loss of the power. It is interesting to note how these unfavorable scenarios are not localized to a certain region or corner of the floor plan but rather exist in "spots," strengthening the notion that the DLOS path can be lost in locations that system designers might have not predicted because of additional obstacles apart from the walls.

IV. TOA Estimation Algorithms

A. IFT

A simple and conventional TOA estimation algorithm, IFT provides a time-domain representation of the channel profile from the frequency-domain measurement data. When the time-domain response over part of the time period is desired, the chirp-z transform (CZT) is preferred, providing flexibility in the choice of time-domain parameters with the cost of longer computational time, as compared with the IFT. As mentioned earlier, a Hanning window is also used to avoid leakage and false peaks by reducing the sidelobes of the time-domain response at the cost of reduced resolution. The peak detection algorithm then selects the first peak above a certain noise threshold. In this paper, the term IFT will generally mean the application of the CZT, unless otherwise stated.

B. DSSS

Another estimation algorithm uses cross-correlation techniques with DSSS signals. To simulate the DSSS signal-based cross-correlation technique, the frequency response of a raised-cosine pulse with a rolloff factor of 0.25 is first applied to the frequency-domain response as a combined response of band-limitation pulse-shaping filters of the transmitter and receiver. Then, the resultant frequency response is converted to time-domain response using the IFT for TOA estimation.

C. Superresolution [EV/Forward-Backward Correlation Matrix (FBCM)]

In this paper, a form of MUSIC algorithm is used as a super-resolution technique in TOA estimation for indoor geolocation [9]. The indoor radio channel suffers from severe multipath, and the equivalent low-pass impulse response is given by

$$h(t) = \sum_{k=0}^{L_p-1} \alpha_k \delta(t - \tau_k) \tag{1}$$

where L_p is the number of multipath components, and $\alpha_k = |\alpha_k| e^{j\theta k}$ and τ_k are the complex attenuation and propagation delay of the kth path, respectively. The Fourier transform of (1) is the frequency-domain channel response, which is given by

$$H(f) = \sum_{k=0}^{L_p-1} \alpha_k e^{-j2\pi f \tau_k}. \tag{2}$$

A harmonic signal model can be created by exchanging the role of the time and frequency variables in (2), which yields

$$H(\tau) = \sum_{k=0}^{L_p-1} \alpha_k e^{-j2\pi f_k \tau}. \tag{3}$$

This model is well known in the spectral estimation field [13]. Therefore, any spectral estimation techniques that are suitable for the harmonic model can be applied to the frequency response of the multipath indoor radio channel to perform time-domain analysis. In this case, the MUSIC algorithm is used as a spectral estimation technique to convert the frequency-domain data to the time-domain profile that is needed to determine the DLOS path and TOA. The discrete measurement data are obtained by sampling the channel frequency response $H(f)$ at L equally spaced frequencies. Considering additive white noise in the measurement, the sampled discrete frequency-domain channel response is given by

$$\begin{aligned} x(l) &= H(f_l) + w(l) \\ &= \sum_{k=0}^{L_p-1} \alpha_k e^{-j2\pi(f_0 + l\Delta f)\tau_k} + w(l) \end{aligned} \tag{4}$$

where $l = 0, 1, \ldots, L-1$, and $w(l)$ denotes additive white measurement noise with zero mean and variance $(\sigma_w)^2$. The signal model in vector form is

$$\mathbf{x} = \mathbf{H} + \mathbf{w} = \mathbf{V}\mathbf{a} + \mathbf{w} \tag{5}$$

where $\mathbf{V} = [\mathbf{v}(\tau_0) \quad \mathbf{v}(\tau_1) \quad \cdots \quad \mathbf{v}(\tau_{L_p-1})]^T$, and $\mathbf{v} = [1 \quad e^{-j2\pi\Delta f \tau k} \quad \cdots \quad e^{-j2\pi(L-1)\Delta f \tau k}]^T$. The MUSIC superresolution algorithm is based on the eigendecomposition of the autocorrelation matrix of the signal model in (5). The autocorrelation matrix is given by

$$\mathbf{R}_{\mathrm{xx}} = E\{\mathbf{x}\mathbf{x}^H\} = \mathbf{V}\mathbf{A}\mathbf{V}^H + \sigma_w^2 \mathbf{I} \tag{6}$$

where $\mathbf{A} = E\{\mathbf{a}\mathbf{a}^{\mathbf{H}}\}$, and the superscript H indicates the Hermitian conjugate transpose of a matrix. Therefore, the L-dimensional subspace that contains signal vector $\mathbf{x}$ is split into two orthogonal subspaces, which are known as signal subspace and noise subspace, by the signal EVs and noise EVs, respectively. Since vector $\mathbf{v}(\tau_k)$, $0 \le k \le L_p - 1$ must lie in the signal subspace, we have

$$\mathbf{P}_w \mathbf{v}(\tau_k) = 0 \tag{7}$$

where $\mathbf{P}_w \mathbf{v}(\tau_k)$ is the projection matrix of the noise subspace. Thus, the multipath delays τ_k, $0 \le k \le L_p - 1$ can be determined by finding the delay values, at which the following MUSIC pseudospectrum achieves the maximum value:

$$\begin{aligned} S_{\mathrm{MUSIC}}(\tau) &= \frac{1}{\|\mathbf{P}_w \mathbf{v}(\tau)\|^2} \\ &= \frac{1}{\sum_{k=L_p}^{L-1} |\mathbf{q}_k \mathbf{v}(\tau)|^2} \end{aligned} \tag{8}$$

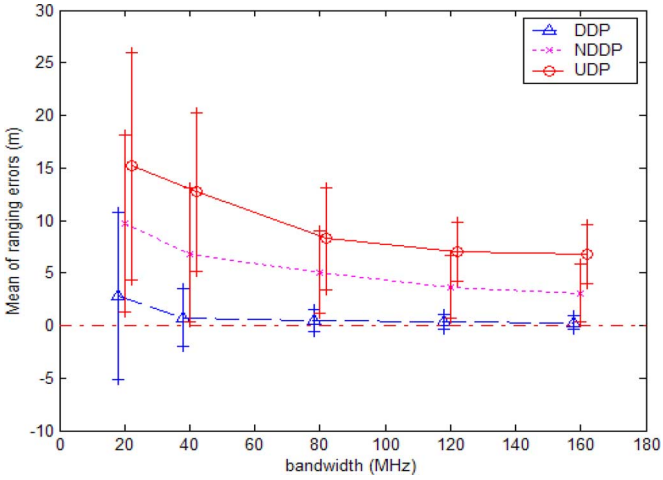

Fig. 4. Mean and STD of ranging errors for DDP, NDDP, and UDP using the IFT algorithm.

where $\mathbf{q}_k$ are the noise EVs. In practical implementation, when only one snapshot of length N is available, the data sequence is divided into M consecutive segments of length L, and then, the estimate of the correlation matrix is further improved using the FBCM that was described in [9]. In this paper, a slight variation on the MUSIC algorithm is used, which is known as the EV method. The pseudospectrum is defined as

$$S_{\mathrm{EV}}(\tau) = \frac{1}{\sum_{k=L_p}^{L-1} \frac{1}{\lambda_k} |\mathbf{q}_w^H \mathbf{v}(\tau)|^2} \tag{9}$$

where λ_k, $L_p \le k \le L-1$ are the noise eigenvalues. Effectively, the pseudospectrum of each EV is normalized by its corresponding eigenvalue. The performance of the EV method is less sensitive to an inaccurate estimate of parameter L_p, which is highly desirable in practical implementations [13]. In this paper, the EV method with FBCM was used to estimate the TOA of the DLOS path. EV/FBCM refers to the type of MUSIC algorithm that is applied throughout this paper, unless otherwise stated.

V. Behavior of Algorithms in Different Environments

From the previous sections, it was clear that UDP is a serious problem for indoor geolocation applications. The measurement campaign showed that indeed this troublesome phenomenon occurs with high probability. The existence of metallic cabinets that might be installed after the geolocation system has been deployed will substantially affect the performance. In this section, a quantitative analysis will show the extent that UDP affects TOA estimation errors and the possible ways to mitigate the problem.

A. Evaluation of Distance Error in UDP Conditions

Fig. 4 shows how the mean and standard deviation (STD) of the ranging error for UDP are substantially larger when compared with the other cases using the IFT algorithm. In fact,

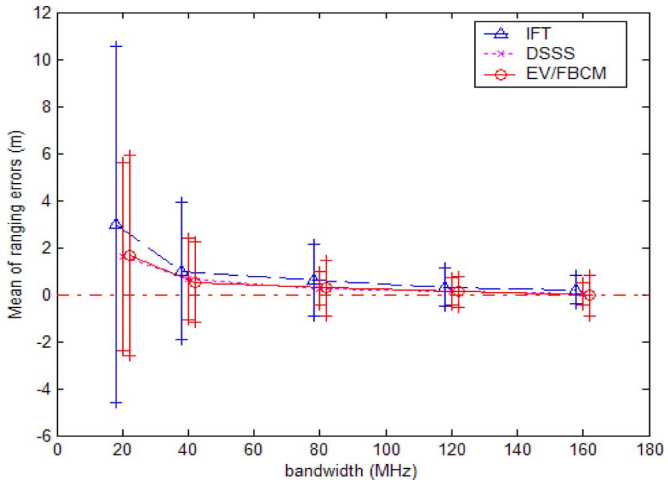

Fig. 5. Mean and STD of ranging errors for DDP using different TOA estimation algorithms. The vertical lines correspond to ± 1 STD about the mean.

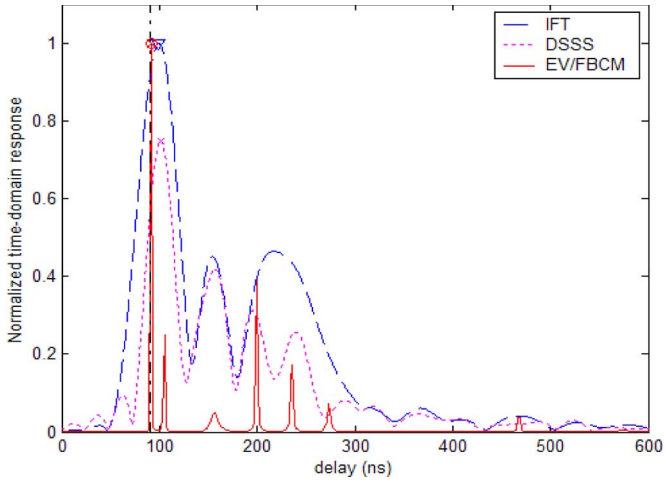

Fig. 6. Measured DDP profile obtained with the three estimation algorithms at 40 MHz.

at 20 MHz, it has a mean error that is five times that of DDP and 1.5 times that of NDDP. Note how the distance error decreases as the bandwidth increases. For example, at 160 MHz, the mean of the distance error for UDP is almost 7 m, while DDP is a mere 0.29 m. Again, these are due to higher bandwidths having higher resolutions in the time domain and, thus, lower error values. While the other channel cases tend to approach zero error as the bandwidth increases, UDP seems to level off at a certain error. Better TOA estimation algorithms reduce the average distance error but have limitations for UDP. The loss of the DLOS path creates a situation where a large distance error is unavoidable, even with an increase in the bandwidth of the system.

B. Performance of TOA Estimation Algorithms in Different Multipath Conditions

The algorithms' abilities to resolve multipath and enhance the time-domain channel profile vary from one condition to another. Fig. 5 shows the mean and STD of the ranging errors for the DDP condition. The algorithms exhibit similar performances, particularly, at higher bandwidths. The strong DLOS path facilitates its detection and the reduction in the distance error. To further analyze this case, Fig. 6 shows a measurement sample of a DDP channel profile at 40 MHz, illustrating the performance of the three algorithms. The vertical dash–dotted line is the expected TOA. Notice that the DLOS is detected successfully for the three algorithms.

For NDDP cases, Fig. 7 shows that the EV/FBCM algorithm performs significantly better than the other two algorithms. In this category, the DLOS path usually combines with the subsequent paths and forms a cluster. The conventional algorithms detect the peak of the cluster as the DLOS path. This erroneous detection causes serious problems for TOA estimation. The higher resolution of the EV/FBCM algorithm "splits" the cluster and estimates other paths that were not detected conventionally. In some cases, the algorithm detects the DLOS path; in other cases, the second or even the third is detected. Regardless of the path detected, Fig. 7 shows that, on average, EV/FBCM

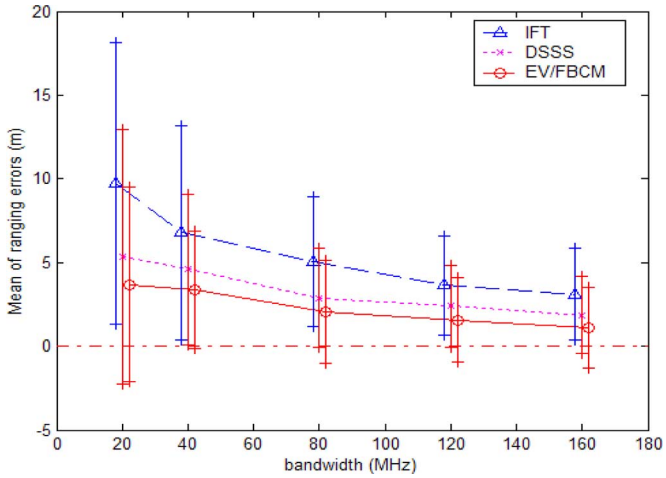

Fig. 7. Mean and STD of ranging errors for NDDP using different TOA estimation algorithms.

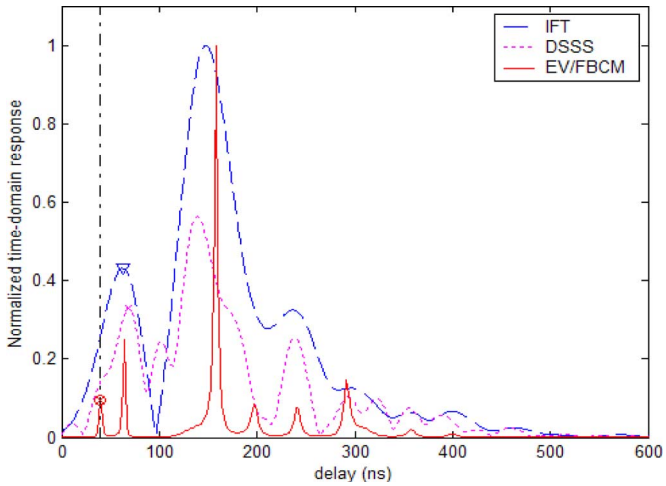

Fig. 8. Measured NDDP profile obtained with the three estimation algorithms at 40 MHz.

exhibits the lower mean of the ranging error when compared with the other algorithms. This performance can be justified by examining Fig. 8, which shows a typical measured NDDP

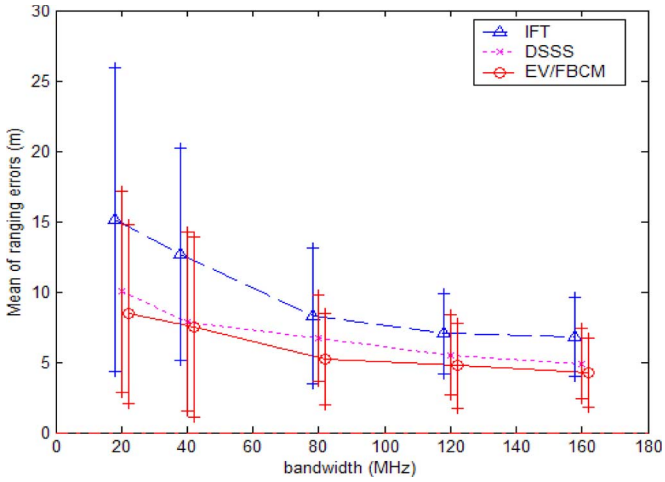

Fig. 9. Mean and STD of ranging errors for UDP using different TOA estimation algorithms.

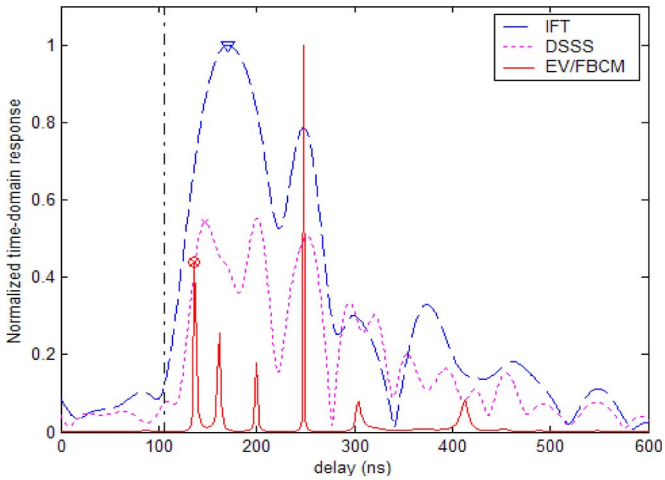

Fig. 10. Measured UDP profile obtained with the three estimation algorithms at 40 MHz.

profile at a system bandwidth of 40 MHz. The vertical dash–dotted line is the expected TOA, and it is clear how both the IFT and the DSSS are unable to detect the correct path. Overall, it is true to say that, in NDDP conditions, EV/FBCM provides the best performance in terms of the mean of ranging errors.

In UDP scenarios, EV/FBCM provides an advantage relative to the other algorithms. Although the DLOS path does not exist, nevertheless, EV/FBCM is expected to perform better than the other algorithms. Fig. 9 shows the mean and STD of the ranging error for UDP conditions. On average, the EV/FBCM outperforms the other algorithms and exhibits lower error, even at higher bandwidths. By examining Fig. 10, it is possible to see how the three algorithms compare. In the absence of the DLOS path, it is clear that EV/FBCM detects a closer path and improves the TOA estimation when compared with other algorithms. The weakness of the DLOS path makes it difficult to resolve the multipath and detect it. As a result, the UDP condition introduces unavoidable errors, and regardless of the bandwidth or the estimation algorithm used, the positioning system will exhibit substantially large errors. This degraded

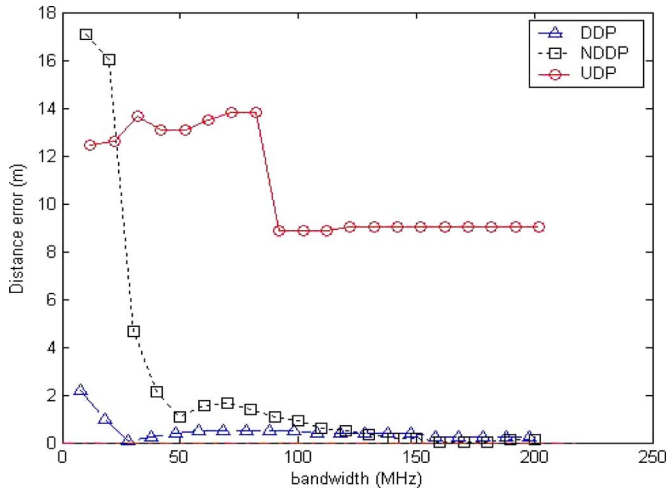

Fig. 11. Measured UDP distance error versus system bandwidth for the different multipath conditions.

performance requires that, in the deployment of an indoor geolocation system, care must be taken to avoid coverage areas with UDP conditions. This will further reduce the error and enhance the accuracy of TOA detection and estimation. Alternatively, cooperative localization can depend on multiple measurements to different sensors, thereby establishing some kind of spatial diversity to mitigate the error that was introduced by this condition.

C. *Effect of System Bandwidth on TOA Error in UDP*

Finally, after assessing the performance of the different estimation algorithms and their effect on the multipath conditions, it is important to analyze the effect of system bandwidth on UDP. A general fact that has been noticed in the analysis section is that, as the bandwidth of the system increases, the estimation error decreases due to enhanced time-domain resolution. For the other conditions, the system bandwidth significantly enhances the estimation of the DLOS path. Fig. 11 shows a plot of the absolute distance error for the three multipath conditions with varying system bandwidths. Note that the ranging error in DDP conditions drops to values below 2 m and then drops significantly after 30 MHz. For NDDP, the error drops from 18 m to about 1.5 m at 50 MHz. As the bandwidth reaches 200 MHz, the error rolls off to zero. Unfortunately, such encouraging results cannot be concluded for UDP. The increases in bandwidths have limited effects. In fact, after 100 MHz, the error stays around the same value of 8.5 m, which is a very significant deficiency in indoor geolocation. As a result, it is possible to see that this adverse condition introduces serious problems in detecting the DLOS path. Finally, it is evident that the bandwidth of the system has limitations in improving the TOA estimation error, particularly for UDP.

VI. Conclusion

In this paper, the behavior of TOA estimation algorithms and the effect of different multipath conditions have been analyzed. A measurement campaign that is targeted at gathering UDP

indoor channel profiles helped in establishing a comprehensive database for statistical analysis in different multipath conditions. In DDP, the performance of the estimation algorithms was very close to each other, and the introduction of advanced estimation algorithms does not provide any advantage. Due to multipath, NDDP scenarios introduce a larger margin of error when compared to DDP and can create significant inaccuracies in TOA estimation. It is possible to see that, in this case, resolving the multipath and detecting the DLOS path are achievable with EV/FBCM, as it offers the best performance in this category. UDP showed the worst algorithm performance. Increasing the bandwidth of the system can improve the accuracy of TOA estimation if the DLOS path is detected. More importantly, the substantial errors that were introduced by UDP conditions are unavoidable, even by increasing the bandwidth of the system and using complex TOA estimation algorithms.

The occurrence of a large ranging error in indoor environments, due to the UDP condition, is a limiting factor to accurate localization. The ability to detect and mitigate this situation in real-time measurements is the next challenge in improving indoor localization performance. To this end, statistical analysis of time-domain channel parameters such as rms delay spread, the ratio of the power of the first detected path versus the strongest path, and the clustering of the neighboring arriving paths to the DLOS could all provide important characterization of the UDP condition. Such research efforts would focus on collecting more measurements and analyzing, statistically, the difference in behavior of the aforementioned parameters in each of the channel categories. In the end, a mobile user would estimate the channel parameters and, from that information, assess the quality of the range estimate and the probability of being in UDP. Finally, extensive measurements and modeling of the ranging error in different building structures and scenarios (e.g., outdoor–indoor and indoor–indoor propagation) are needed to design reliable and accurate indoor geolocation systems.

REFERENCES

[1] M. J. Meyer *et al.*, "Wireless enhanced 9-1-1 service—Making it a reality," *Bell Labs Tech. J.*, vol. 1, no. 2, pp. 188–202, Autumn 1996.

[2] K. Pahlavan, P. Krishnamurthy, and J. Beneat, "Wideband radio propagation modeling for indoor geolocation applications," *IEEE Commun. Mag.*, vol. 36, no. 4, pp. 60–65, Apr. 1998.

[3] K. Pahlavan and A. Levesque, *Wireless Information Networks*. New York: Wiley, 1995.

[4] K. Pahlavan, X. Li, and J. Makela, "Indoor geolocation science and technology," *IEEE Commun. Mag.*, vol. 40, no. 2, pp. 112–118, Feb. 2002.

[5] H. Yamada, M. Ohmiya, Y. Ogawa, and K. Itoh, "Superresolution techniques for time-domain measurements with a network analyzer," *IEEE Trans. Antennas Propag.*, vol. 39, no. 2, pp. 177–183, Feb. 1991.

[6] W. Beyene, "Improving time-domain measurements with a network analyzer using a robust rational interpolation technique," *IEEE Trans. Microw. Theory Tech.*, vol. 49, no. 3, pp. 500–508, Mar. 2001.

[7] T. Lo, J. Litva, and H. Leung, "A new approach for estimating indoor radio propagation characteristics," *IEEE Trans. Antennas Propag.*, vol. 42, no. 10, pp. 1369–1376, Oct. 1994.

[8] G. Morrison and M. Fattouche, "Super-resolution modeling of the indoor radio propagation channel," *IEEE Trans. Veh. Technol.*, vol. 47, no. 2, pp. 649–657, May 1998.

[9] X. Li and K. Pahlavan, "Super-resolution TOA estimation with diversity for indoor geolocation," *IEEE Trans. Wireless Commun.*, vol. 3, no. 1, pp. 224–234, Jan. 2004.

[10] S. J. Howard and K. Pahlavan, "Measurement and analysis of the indoor radio channel in the frequency domain," *IEEE Trans. Instrum. Meas.*, vol. 39, no. 5, pp. 751–755, Oct. 1990.

[11] E. Zand, "Measurement of TOA using frequency domain techniques for indoor geolocation," M.S. thesis, Worcester Polytechnic Inst., Worcester, MA, 2003.

[12] J. Beneat, K. Pahlavan, and P. Krishnamurthy, "Radio channel characterization for geolocation at 1 GHz, 500 MHz, 90 MHz and 60 MHz in SUO/SAS," in *Proc. IEEE MILCOM*, 1999, pp. 1060–1063.

[13] D. Manolakis, V. Ingle, and S. Kogon, *Statistical and Adaptive Signal Processing*. New York: McGraw-Hill, 2000.

[14] K. Pahlavan and P. Krishnamurthy, *Principles of Wireless Networks—A Unified Approach*. Englewood Cliffs, NJ: Prentice-Hall, 2002.

Nayef Alsindi (S'02) received the B.S.E.E. degree from the University of Michigan, Ann Arbor, in 2000 and the M.S. degree in electrical engineering from Worcester Polytechnic Institute (WPI), Worcester, MA, in 2004. He is currently working toward the Ph.D. degree in electrical and computer engineering with the Center for Wireless Information Network Studies, Department of Electrical and Computer Engineering, WPI.

From 2000 to 2002, he was a Technical Engineer with Bahrain Telecom. From 2002 to 2004, he was awarded a Fulbright Scholarship to pursue the M.S. degree at WPI. His research interests include performance limitations of time-of-arrival-based ultra-wide band ranging in indoor non-line-of-sight (LOS) conditions, cooperative localization for indoor wireless sensor networks, and non-LOS/blockage identification and mitigation.

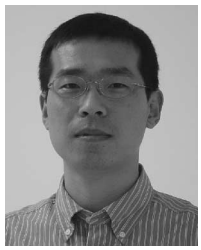

Xinrong Li (S'00–M'04) received the B.E. degree from the University of Science and Technology of China, Hefei, China, in 1995, the M.E. degree from the National University of Singapore, Singapore, in 1999, and the Ph.D. degree from Worcester Polytechnic Institute (WPI), Worcester, MA, in 2003, all in electrical engineering.

From 2003 to 2004, he was a Postdoctoral Research Fellow with the Center for Wireless Information Network Studies, Department of Electrical and Computer Engineering, WPI. Since 2004, he has been with the Department of Electrical Engineering, University of North Texas, Denton, as an Assistant Professor. His current research interests include statistical signal processing for geolocation, wireless communications, and sensor networks.

Kaveh Pahlavan (M'79–SM'88–F'96) received the B.S. and M.S. degrees from the University of Tehran, Tehran, Iran, in 1975 and the Ph.D. degree from Worcester Polytechnic Institute, Worcester, MA, in 1979, all in electrical engineering. He is currently a Professor of electrical and computer engineering, a Professor of computer science, and the Director of the Center for Wireless Information Network Studies, Department of Electrical and Computer Engineering, Worcester Polytechnic Institute. He is also a Visiting Professor with the Telecommunication Laboratory and Center for Wireless Communications, University of Oulu, Oulu, Finland. He is a coauthor of the *Wireless Information Networks* (Wiley, 1995) (with A. Levesque) and *Principles of Wireless Networks—A Unified Approach* (Prentice-Hall, 2002) (with P. Krishnamurthy).

Prof. Pahlavan is the Editor-in-Chief of the *International Journal of Wireless Information Networks*, a member of the advisory board of the *IEEE Wireless Magazine*, a member of the executive committee of the IEEE PIMRC, a 1999 Nokia Fellow, and a 2000 Fulbright–Nokia Scholar. He has served as the general chair and organizer of a number of successful IEEE events and has contributed to numerous seminal technical and visionary publications in wireless office information networks, home networking, and indoor geolocation science and technology.